COHERENT HARMONIC GENERATION USING THE ELETTRA STORAGE-RING OPTICAL KLYSTRON: A NUMERICAL ANALYSIS

F. Curbis*, University of Trieste & Sincrotrone Trieste, G. De Ninno, Sincrotrone Trieste

Abstract

Coherent harmonic generation can be obtained by means of frequency up-conversion of a high-power external laser focused into the first undulator of an optical klystron. The standard configuration is based on a single-pass device, where the seed laser is synchronized with an electron beam entering the first undulator of the optical klystron after being accelerated using a linear accelerator. As an alternative, the optical klystron may be installed on a storage ring, where it is normally used as interaction region for an oscillator free-electron laser. In this case, removing the optical cavity and using an external seed, one obtains a configuration which is similar to the standard one but also presents some peculiar characteristics. In this paper we investigate the possibility of harmonic generation using the Elettra storage-ring optical klystron. We explore different experimental set-ups varying the beam energy, the seed characteristics and the strength of the optical-klystron dispersive section. We also study the coherent/incoherent signal ratio for different harmonics. Numerical simulations are performed using the numerical code `Genesis`.

INTRODUCTION

The process leading to Coherent Harmonic Generation (CHG) using an optical klystron (OK) is induced by a temporally and transversely coherent input signal from conventional laser in the ultraviolet region (200-300 nm). The interaction between such a seed and a synchronized electron beam entering the first undulator (modulator) of the OK leads to a modulation of the electrons energy. When the beam crosses the dispersive section, such a modulation is converted into a spatial partition of the electrons in micro bunches separated by the seed wavelength (microbunching). Finally, in the second undulator (radiator), the light emission is enhanced by this coherent bunching and becomes proportional to the square of the number of electrons. CHG can be performed using oscillators or single-pass devices. In the first configuration, the seeding signal which induces the coherent emission is provided by the free-electron laser (FEL) light stored in a optical cavity [1]. The second configuration, which needs an external laser, is normally implemented on linac-based FELs [4, 5, 6]. However, after removing the mirrors of the optical cavity, also a storage-ring FEL may be suited for single-pass CHG [2, 3]. In this case the radiator is generally too short to reach saturation and, as a consequence, less output power is to be expected with respect to linac-based devices. Moreover, in the case of a storage ring, electrons are re-circulated and not renewed after each pass through the OK, as in a single-pass configuration. After each interaction with the seed laser, the electron beam needs few synchrotron damping times (order of tens of milliseconds) to cool down. This time interval determines the maximum achievable repetition rate (few Hz) for this configuration.

A storage-ring FEL is currently operational at Sincrotrone Trieste in the visible-VUV spectral range [7, 8]. It relies on Elettra, a third-generation synchrotron radiation facility, characterized by a high-quality electron beam and a wide operational energy range. The main characteristics of the source can be found in Table 1. In this paper we show that the Elettra storage-ring FEL can be transformed in an appealing and (almost) ready-to-use test facility for CHG experiments planned on next generation single-pass devices. For this purpose, we present a campaign of simulations aimed at comparing different experimental set-ups. This includes the comparison between several working points (in terms of electron-beam energy, emittance, Twiss parameters, seed power, strength of the dispersive section), the aim being the maximization of the extracted harmonic power. The sensitivity of the system performance to electron-beam energy spread is studied and compared with theoretical predictions [4]. The problem of the maximization of the signal-to noise ratio is also addressed. Simulations have been performed using the 3-D numerical code `Genesis` [9].

OPTIMIZATION OF THE EXPERIMENTAL SETUP

Consider the following modification to the standard configuration of the Elettra storage-ring FEL (see Figure 1): the optical cavity is removed and use is made of an external seed synchronized with the electron beam circulating into the ring. We have performed a set of simulations assuming the following nominal setup. A current per bunch of 6 mA, corresponding to a peak power of 77 A (at 0.9 GeV); a seed, e.g., a Ti:Sapphire-based system, delivering an optical pulse at 240 nm having a duration of 100 fs and a maximum peak power of 2.5 GW [10]. The modulator is tuned at the seed wavelength and the strength of the dispersive section is chosen so to maximize the electron-bunch harmonic content at the entrance of the radiator. The radiator is tuned at the third harmonic (i.e. 80 nm) of the seeding signal. As show in Table 1, the Elettra SRFEL can be operated in the electron-beam energy range between 0.75 and 1.5 GeV. In Figure 2 one can follow the behavior of the maximum extracted power at 80 nm as a function of the seed power for three different energies, i.e. 0.75, 0.9 and

* francesca.curbis@elettra.trieste.it

Table 1: Main Elettra FEL parametres

Electron beam	
Energy	0.75-1.5 GeV
Maximum bunch current	6 mA
No. of circulating e-bunches	4
Emittance RMS at 0.9 GeV	1.53 nm rad
Natural RMS energy-spread	0.036% at 0.9 GeV 0.030% at 0.75 GeV 0.060% at 1.5 GeV
Natural RMS bunch-length	at 0.9 GeV 5.4 ps 4.1 ps at 0.75 GeV 11.6 ps at 1.5 GeV
RMS energy-spread at 6 mA	0.12% at 0.9 GeV 0.23% at 0.75 GeV 0.08%at 1.5 GeV
RMS bunch-length at 6 mA	27 ps at 0.9 GeV 28 ps at 0.75 GeV 25 ps at 1.5 GeV
FEL characteristics	
Spectral range	visible-176 nm
Pulse duration	$\leq$10 ps
Interpulse period	216 ns
Relative spectral width	$\leq 4 \cdot 10^{-4}$
Extracted average power	few mW - 500 mW
Extracted peak power	2 kW

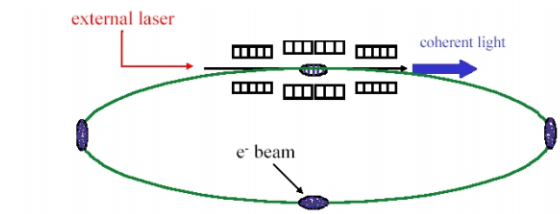

Figure 1: Layout of Elettra storage-ring FEL after removing the optical cavity and making use of an external seed laser for inducing CHG.

1.5 GeV. It is first of all worth stressing that, no matter the energy, the maximum harmonic power corresponds to the maximum seed. This is mainly due to the fact that the uncorrelated energy spread is quite high (see Table 1) and, as a consequence, a strong seed is required for inducing a significant energy modulation inside the modulator. This point deserves a deeper analysis. For this purpose, let's consider the analytical model proposed by L.H.Yu in [4]. According to such a model, the behavior of the harmonic electric field along the radiator in the limit of vanishing energy spread is:

$$E = \frac{4\sqrt{2}mc^2 k_s k_w}{e} \cdot A_0 \rho z. \qquad (1)$$

Here m and e are the electron rest mass and the charge respectively, c is the light speed, k_s is the radiation filed wave number, k_w is the wiggler field wave number, ρ is

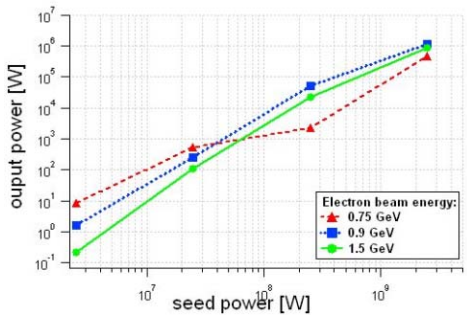

Figure 2: Maximum output power vs. seed power for three energies.

the Pierce parameter, $A \propto \rho^2\gamma^2 b$ (γ being the electron beam-energy in terms of the electron rest mass energy and b the bunching factor) and z is the length along the radiator. Note that Eq. 1 is valid when the peak power[1] varies quadratically with z. Due to the short undulator length, this is indeed the dynamical regime we are interested in. Now, considering that ρ is proportional to $1/\gamma$, the lower the energy the higher the power. This result is shown in Figure 3 and confirmed by numerical simulations performed assuming for the energy spread and the bunch length the natural values reported in Table 1. If the energy spread at 6 mA is

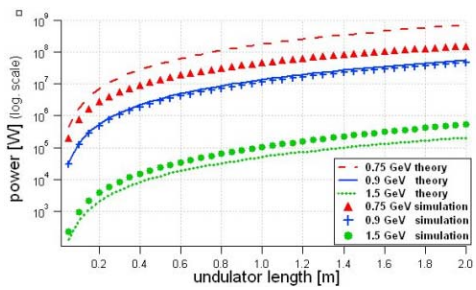

Figure 3: Power vs. undulator length assuming for the energy spread and the bunch length the natural values reported in Table 1.

used instead, the amplification gain decreases [11] and, as a consequence, one observes a diminution of the harmonic output power. The fact that the energy spread at the working electron-beam current is higher at lower energies (see Table 1) may determine an inversion of the trend predicted by Yu's model (see Figure 3). Indeed, as shown in Figure 4, the power obtained at 0.9 GeV overcomes the one obtained at 1.5 GeV.

CHG PERFORMANCE

Given the setting described above and concentrating on the case at 0.9 GeV (which is the most promising), we report in the following the results of a campaign of time-

[1]The peak power is proportional to the square of the electric field according to the following relation: $P = \frac{\pi}{2} w_0^2 c \epsilon_0 E^2$, where w_0 is the laser beam waist and ϵ_0 is the vacuum permittivity.

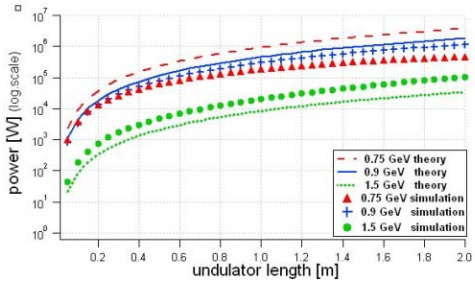

Figure 4: Power vs. undulator length assuming for the energy spread and the bunch length the values corresponding to an electron-beam current of 6 mA (see Table 1).

dependent simulations carried out using the numerical code `Genesis` [9]. Figure 5 displays the behavior of the harmonic peak power along the radiator (tuned at 80 nm). The result is in agreement with the one reported in previous Section (see Figure 4). Figure 6 and Figure 7 show, respectively, the output temporal profile and spectrum of the harmonic radiation.

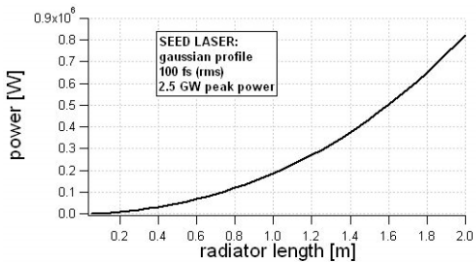

Figure 5: Power vs. radiator length. Time dependent simulation using the numerical code `Genesis`. The electron-beam and seed temporal profiles have been assumed to be Gaussian. The seed has a duration of 100 fs, a peak power of $2.5 \cdot 10^9$ W and is centred at 240 nm. The radiator is tuned on the third harmonic of the seed (i.e. 80 nm). The other input parameters are listed in Table 1.

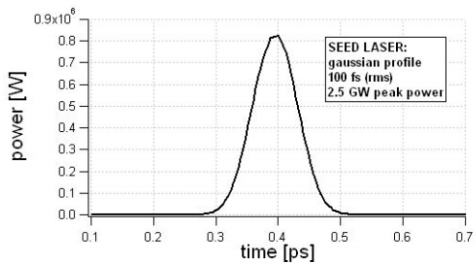

Figure 6: Temporal profile of the harmonic signal at the exit of the radiator. Pulse duration (rms): $\sim 72\ fs$.

Sensitivity to seed pulse profiles

We checked the influence of the seed pulse shape on the output harmonic signal. For this purpose, three different profiles have been considered, besides the gaussian one [12], i.e. box, increasing and decreasing shapes. Figure 8 and Figure 9 show all the input seed profiles, whereas in Figure 10 and in Figure 11 the pulse temporal profile and the spectrum are displayed for all shapes at the end of the radiator. The input peak power, in the all four cases is 2.5 GW and for the increasing and decreasing shapes the function used is an exponential. Compared to the gaussian shape, the others give less output power and the spectrum is more spiky and broad. The Gaussian profile seems to be therefore preferable.

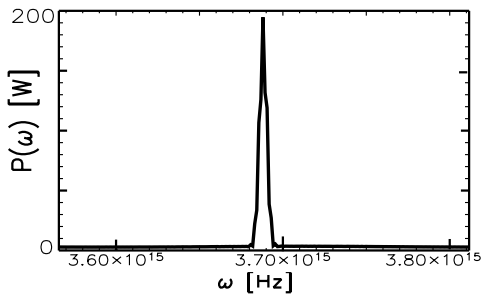

Figure 7: Spectrum of the harmonic signal at the exit of the radiator. Relative spectral width (rms): $\sim 0.5 \cdot 10^{-3}$.

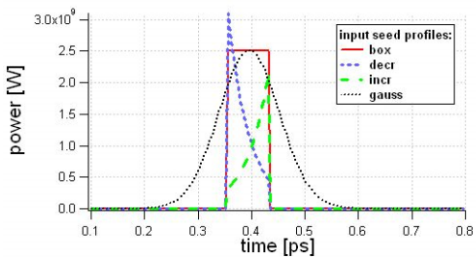

Figure 8: Seed profiles having different shapes.

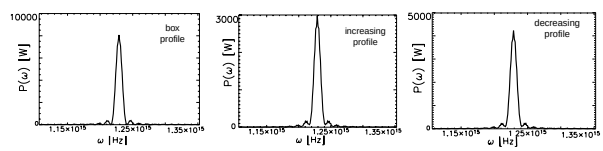

Figure 9: Spectrum of the harmonic signal at the exit of the modulator: box shape (left), increasing shape (center), decreasing shape (right).

Signal-to-noise ratio

The single-shot harmonic signal experimentally detected at a given wavelength will result from the superposition of two contributions: a coherent one, provided by the electrons whose energy is modulated due to the interaction with the external laser, and an incoherent one, generated by the electrons which are not involved in the interaction. The ratio between these two contributions can be calculated using

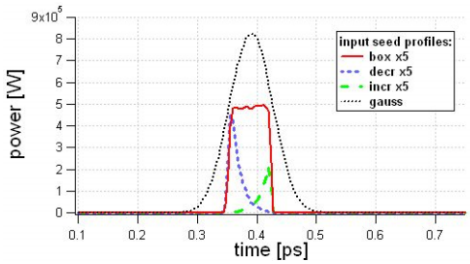

Figure 10: Output temporal profiles of the harmonic pulse corresponding to different seed shapes.

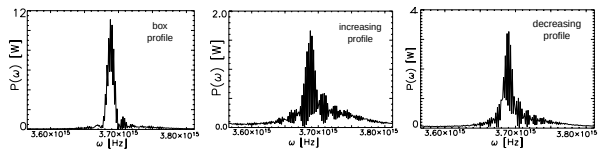

Figure 11: Spectrum of the harmonic signal at the exit of the radiator: box shape (left), increasing shape (center), decreasing shape (right).

the relation [13, 14]:

$$R = \frac{N_{eff}^2}{2N_{tot}^2} \cdot J_n[4\pi n(N+N_d)\frac{\Delta\gamma}{\gamma}]^2 \cdot e^{-[4\pi n(N+N_d)\frac{\sigma_\gamma}{\gamma}]^2} \quad (2)$$

where N_{eff} is the number of electrons in the bunch directly involved in the micro-bunching process, N_{tot} is the total number of electrons in the bunch, N_d is the number of dispersive section equivalent periods, $\frac{\Delta\gamma}{\gamma}$ is the coherent electron energy spread induced by the seed laser and $\frac{\sigma_\gamma}{\gamma}$ is the rms incoherent energy spread before the interaction with the laser. Using a seed laser characterized by a peak power of 2.5 GW and a pulse duration of 200 fs, the values of R for different harmonics are calculated and reported in Table 2.

As already mentioned, the repetition rate at which storage-ring CHG can be performed is quite low (few Hz). This implies that the incoherent contribution to the detected signal at a given wavelength is strongly enhanced (and, as a consequence, the parameter R strongly reduced) by all the non-seeded bunches passing through the OK. For maintaining a significantly high signal-to-noise ratio a gating procedure (e.g. a chopper) is to be envisaged.

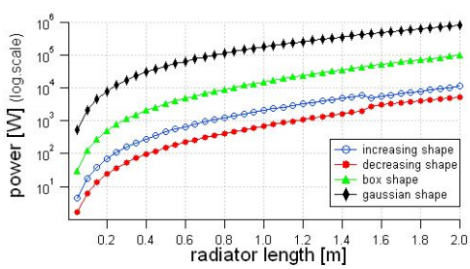

Figure 12: Output power vs. radiator length for all four pulse shapes.

Table 2: Calculated ratios between coherent and incoherent emission for the third, fifth and seventh harmonics.

Coherent/incoherent signal ratio	
Third harmonic	$1.1 \cdot 10^4$
Fifth harmonic	$1.6 \cdot 10^3$
Seventh harmonic	10

CONCLUSIONS

On the basis of the numerical results reported in this paper, we can state that the Elettra storage-ring FEL can be converted into a promising test facility for CHG experiments. The characteristics of the radiation source at 80 nm (third harmonic of seed laser) are listed in Table 3. We also studied the performance at the fifth (48 nm) and seventh ($\sim$ 34 nm) harmonics of the seed laser. We found that, moving from third to fifth harmonic, the extracted power decreases of about one order of magnitude and the same holds when passing from fifth to seventh.

Table 3: Performance of the source at third harmonic (80 nm) of the seed laser. Results have been obtained making use of the electron beam parameters listed in Table 1 and of a seed laser with a peak power of 2.5 GW.

Source performance	
Wavelength	80-100 nm
Maximum extracted power	$\sim 10^6$ W
Pulse duration (rms)	$\sim$ 72 fs
Relative spectral width (rms)	$\sim 0.5 \cdot 10^{-3}$

REFERENCES

[1] V. Litvinenko, Private Communication.

[2] B. Girard et al., *Phys. Rev. Lett.* **62** (1984) 2405.

[3] D. A. Jaroszynski et al., *Phys. Rev. Lett.* **70** (1993) 3412.

[4] L.H.Yu, *Phys. Rev. A* **44** (1991) 5178.

[5] A. Doyuranet al., *Phys. Rev. Lett.* **86** (2001) 5902.

[6] L.H.Yu, *Phys. Rev. Lett.* **91** (2003) 74801.

[7] R. P. Walker, Proc. EPAC'99, 93.

[8] G. De Ninno et al., *Nucl. Instrum. and Meth. A* **483** (2002) 177.

[9] S. Reiche, *Nucl. Instrum.. and Meth. A* **429** (1999) 243.

[10] M. Danailov, Private Communication.

[11] R. Bonifacio, *Il Nuovo Cimento*, vol.13, n.9 (1990).

[12] A. M. Meseck et al., *Proc. 2004 FEL Conf.* 116-119.

[13] P. Ellaume, ESRF int. note(ESRF/MACH ID 99/54)(1999).

[14] R. Coisson, F. De Martini, *Phys.Quant.El.* **9** (1982) 939.